Synthesis of New Self-assembled Pd^{II} and Pt^{II} Rectangular Metallomacrocycles: A Comparative Study of their Inclusion Complexes

Marcos Chas, Dolores Abella, Víctor Blanco, Elena Pía, Gerardo Blanco, Antonio Fernández, Carlos Platas-Iglesias, Carlos Peinador,* and José M. Quintela*[a]

Dedicated to Professor Miguel Yus on the occasion of his 60th birthday

Abstract: New palladium and platinum metallocycles have been synthesized by reacting 4,4′-bipyridinium-based ligands with Pd^{II} and Pt^{II} complexes. Strict thermodynamic self-assembly of **1** and [M(en)(NO₃)₂] (M = Pd, Pt) **6a,b** afforded metallocycles **7a,b**. However, the synthesis of **8a,b** and **9a,b** required a self-assembly process that used sodium *p*-phenylenediacetate (**12**) as a template. Finally, metallocycles **10a,b** were synthesized under high dilution conditions from ligand **4**. The formation of inclusion complexes between metallocycles **7–10** and substrates **13** and **14** were studied by low-temperature ¹H NMR, and the association constants were determined in nitromethane and water by following the characteristic charge-transfer band that these metallomacrocycles show in their UV-visible absorption spectra. A clear correlation between the affinity for a substrate and the dimensions of the metallocycle was observed. Metallocycles **8b** and **9b** exhibited the highest binding constants in water and nitromethane. This observation is in agreement with the DFT (B3LYP)-optimized geometries obtained for the different metallomacrocycles, which indicate that only macrocycles **8** and **9** possess a cavity with a width larger than 3.5 Å. The insertion of hydroquinone or diol **13** into the cavity of metallocycle **11a** was confirmed by single-crystal X-ray crystallography.

Keywords: inclusion compounds · metallocycles · N ligands · self-assembly · supramolecular chemistry

Introduction

Metal-coordination-directed self-assembly of well-defined supramolecular structures is a growing area at the forefront of supramolecular chemistry.[1] In addition to the remarkable self-assembly formation reactions and the unusual structures, metallocyclophanes have attracted attention as a consequence of their potential for use as sensors, probes, photonic devices, and catalysts, as well as in basic host–guest chemistry.[2] In this context, metallocycles, such as molecular triangles, squares, pentagons, and hexagons, have been synthesized over the last few years.[3] Although they can be considered as potential receptors for aromatic systems, rectangular molecular structures have remained relatively rare.[1h, 4]

A very fruitful self-assembly strategy has proven to be the use of palladium and platinum complexes in combination with N ligands. The use of these metal centers with a 4,4′-bipyridine ligand has been especially profitable in the synthesis of 2D and 3D molecular structures.[5] However, the poor π-acceptor ability of 4,4′-bipyridine limits the use of π-acceptor/π-donor interactions for the formation of host–guest complexes based on these types of ligands and forces.

In contrast, the *N,N′*-dialkyl-4,4′-bipyridinium or *N,N′*-dialkyl-2,7-diazapyrenium derivatives show a strong π-deficient character, which has been successfully used by Stoddart and co-workers for the preparation of a myriad of catenanes and rotaxanes.[6] The key step in these processes relies on the electronic complementarity between dialkyl-4,4′-bipyridinium and dioxoaryl components. However, the lack of metal-binding units (nitrogen donor atoms) in di-alkylated 4,4′-bipyridines precludes their use as ligands for the preparation of metallocycles. One approach that we have success-

[a] Dr. M. Chas, D. Abella, V. Blanco, E. Pía, G. Blanco, A. Fernández,
Prof. Dr. C. Platas-Iglesias, Prof. Dr. C. Peinador, Prof.
Dr. J. M. Quintela
Departamento de Química Fundamental
Universidade da Coruña
Facultad de Ciencias
A Zapateira, s/n 15071
La Coruña (Spain)
Fax: (+34) 981-167-065
E-mail: capeveqo@udc.es
jqqoqf@udc.es

Supporting information for this article is available on the WWW under http://www.chemeurj.org/ or from the author.

fully explored in the synthesis of catenanes involves the use of ligands based on *N*-monoalkyl-4,4′-bipyridinium.[7] The formation of a dative bond between these ligands and a palladium or platinum center increases the π-acceptor character of bipyridine rings and directs the self-assembly of [2]- and [3]catenanes.

In view of these recent findings, we became interested in expanding the structural diversity of this type of ligand to be used in the synthesis of new molecular rectangles, which are expected to bind aromatic guests because the predicted interplanar separation is ideal for aromatic intercalation (≈ 3.5 Å). To gain further insight into the factors governing their ability to form supramolecular assemblies, we report herein a comparative study of the complexation properties of different molecular rectangles based on *N*-monoalkyl-4,4′-bipyridinium ligands and Pd^{II} or Pt^{II} centers.

Results and Discussion

The metallomacrocycles described in this work were prepared from ligands **1–5** and complexes **6a,b** (Scheme 1). The
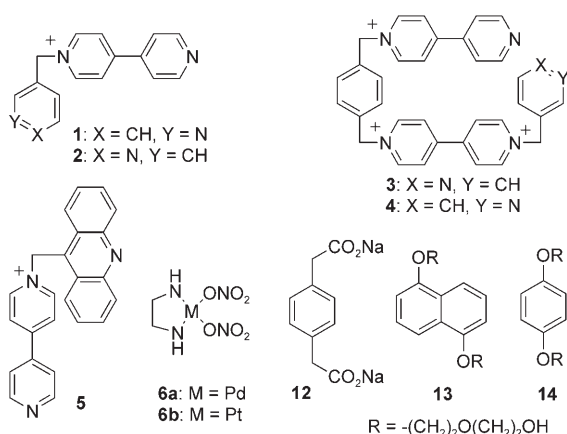
Scheme 1. Structures of ligands **1–5**, metal complexes **6a,b**, and substrates **12–14**.

syntheses of these ligands were achieved by treating 4,4′-bipyridine or 1,1′-[1,4-phenylenebis(methylene)]bis-4,4′-bipyridinium bis(hexafluorophosphate) with the corresponding heterocyclic bromomethyl derivative (3- or 4-bromomethylpyridine and 10-bromomethylacridine). The displacement of the two labile nitrate ligands in the metal complexes **6a,b** by ligands **1–5** in thermodynamically controlled reactions led to the formation of metallocycles **7–11** (Scheme 2).[8]

Self-assembly of Pd^{II} dinuclear metallocycles 7a·6NO$_3$, 8a·6NO$_3$, and 11a·6NO$_3$: The addition of [Pd(en)(NO$_3$)$_2$] (**6a**, 1 equiv) to a solution of ligand **1·NO$_3$** (10 mM) in deuterium oxide produced immediate changes in the ^{1}H and ^{13}C NMR spectra. Proton and carbon signals of the aromatic rings coordinating the palladium(II) center were shifted downfield, in particular those of carbon nuclei in the α posi-
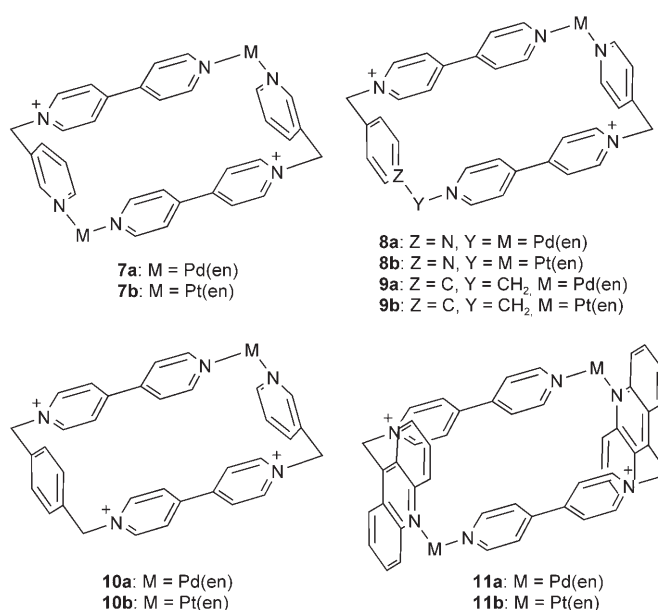
Scheme 2. Structures of the metallocycles studied in this work.

tion relative to the nitrogen, with shifts of up to $\delta = 4$ ppm. These changes are usually observed after the coordination of a pyridinium-based ligand to a palladium(II) (or platinum(II)) metal center, and are attributed to charge transfer from the pyridinium ring to the metal center. To confirm the binding of the pyridinium ligand to the metallic center, we carried out DOSY (diffusion ordered spectroscopy)[9] experiments on a mixture of ligand **1·NO$_3$** and complex **6a**. The results show the formation of a single species in solution with a larger size than that of the reactants, as indicated by the much lower diffusion coefficient shown by all of the NMR signals compared with those of both **1·NO$_3$** and **6a**. The electrospray ionization (ESI) mass spectrum recorded for a solution in MeOH showed an intense signal at $m/z = 540$ that was assigned to $[M-2\,NO_3+2\,CH_3OH]^{2+}$, and which confirms the formation of the desired metallocycle **7a·6NO$_3$**.

The self-assembly process of 1-(pyridin-4-ylmethyl)-4,4′-bipyridin-1-ium (**2·NO$_3$**) and palladium(II) complex **6a** in deuterium oxide is similar to the previous example. In this case, after addition of complex **6a** (1 equiv) to a solution of ligand **2·NO$_3$** (10 mM) in D$_2$O, a set of signals that correspond to a major species in solution was observed in the NMR spectra. The results from these ^{1}H, ^{13}C, bidimensional NMR and DOSY experiments are compatible with the proposed binuclear metallocycle structure **8a·6NO$_3$** (Scheme 2).

However, the NMR spectra also reveal the presence of secondary products in solution at any concentration (Figure 1B). An alternative way of directing the formation of the structure is to exploit the template effect. The proposed structure for metallocycle **8a·6NO$_3$** presents a hydrophobic cavity that is $\approx 3.9 \times 7.0$ Å (see below), which is the ideal size for the inclusion of an aromatic ring. The inclusion of a template molecule or anion in the cavity of the metallocycle may result in the stabilization of the receptor on account of
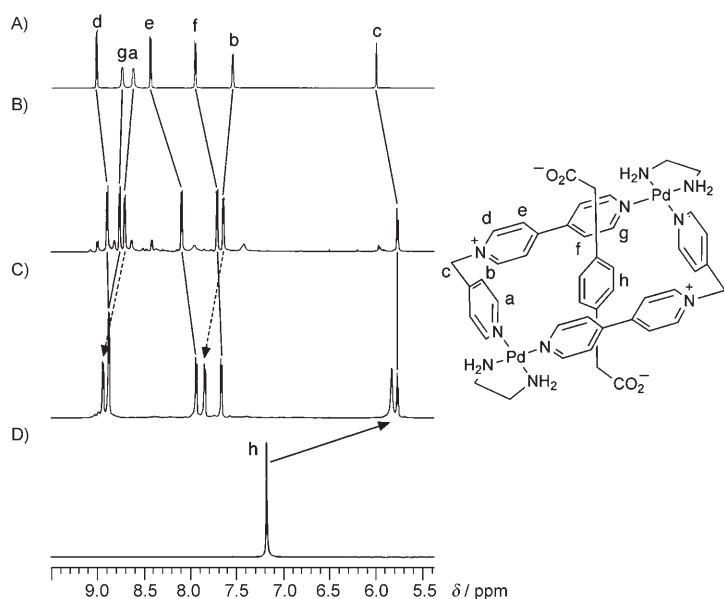
Figure 1. Partial ^{1}H NMR (300 MHz, D$_2$O, 298 K) spectra of: A) 2·NO$_3$; B) a mixture of 2·NO$_3$ (10 mM) and 6a (10 mM); C) a mixture of 2·NO$_3$ (10 mM), 6a (10 mM), and 12 (10 mM); and D) 12.

favorable template–metallocycle interactions, which are responsible for the inclusion process. Disodium *p*-phenylenediacetate (12) has the ideal structural and chemico-physical properties to act as a template for the self-assembly of 8a·6NO$_3$. It is water soluble and possesses an aromatic ring with the ideal dimensions and hydrophobic character for its inclusion in the metallocycle cavity.[10] Moreover, the negatively charged carboxylate groups can be electrostatically attracted by the positive charges of the metallocycle. Another important characteristic is the poorly coordinating character of the carboxylate groups in comparison with the pyridine ligands for coordination to Pd^{II}.

Taking all of these considerations into account, sodium *p*-phenylenediacetate (1 equiv) was added to an equimolecular solution of 2·NO$_3$ (10 mM) and 6a (10 mM). As a result, a reorganization of the system occurred to afford a single species in solution, the NMR spectra of which indicated the insertion of the *p*-phenylenediacetate dianion into the metallocyclic cavity. For example, the resonance of proton H$_h$ in 12 shifts upfield by $\Delta\delta =$ 1.3 ppm (Figure 1), which provides clear evidence for its introduction into the cavity. This shift is a consequence of the hydrogen-bonding interaction between these protons and the perpendicularly oriented pyridine π clouds, the ring currents of which have a shielding effect. The important down-

field shift of the signals attributed to the protons of the pyridine ring (a and b joined by dotted arrows in Figure 1) is also a consequence of their position in the deshielding region of the template ring currents owing to the inclusion of 12 in the macrocyclic cavity. Similar up- and downfield shifts have been previously observed as a result of C−H···π interactions.[4e,11] The other metallocycle signals present slight up- or downfield shifts that are attributed to the influence of the enclosed template anion.

The reaction of acridine ligand 5·NO$_3$ with 6a (1 equiv) afforded a mixture of compounds, as evidenced by the ^{1}H NMR spectrum (see the Supporting Information). Neither dilution (>1 mM) nor addition of 12 or hydroquinone could direct the system towards the formation of a single species in solution.

Synthesis of mononuclear Pd^{II} metallocycles 9a·5NO$_3$ and 10a·5NO$_3$: The ^{1}H NMR spectrum of an equimolecular solution of 6a (10 mM) and 3·3NO$_3$ (10 mM) in D$_2$O shows signals for at least two different species in solution (Figure 2). With the aim of favoring the smallest monomeric metallocycle, we carried out dilution experiments that were monitored by ^{1}H NMR (Figure 2). The resulting spectra show how the proportion of one of the species present in the solution increases as the concentration of the reactants is decreased to 0.5 mM. At this concentration, the ^{1}H NMR spectrum indicated the presence of a single species in solution. The ^{13}C NMR signals of C$_a$ and C$_q$ shift downfield by $\delta = 8.8$ and 10.0 ppm, respectively, with respect to their position in the spectrum of the free ligand. These shifts are attributed to formation of two Pd−N bonds. The spectrum also shows two signals for the carbon nuclei of the ethylenediamine moiety that are in agreement with the expected C_1 symmetry of 9a in solution. The formation of 9a·5NO$_3$ was also confirmed by ESI-MS, which shows peaks that result from the loss of two to four nitrate anions and the addition of a methanol molecule. DOSY experiments (Figure 3) indicate significantly larger diffusion coefficients for 3·3NO$_3$ and 6a than for 9a·5NO$_3$, which supports the formation of the desired metallocycle.
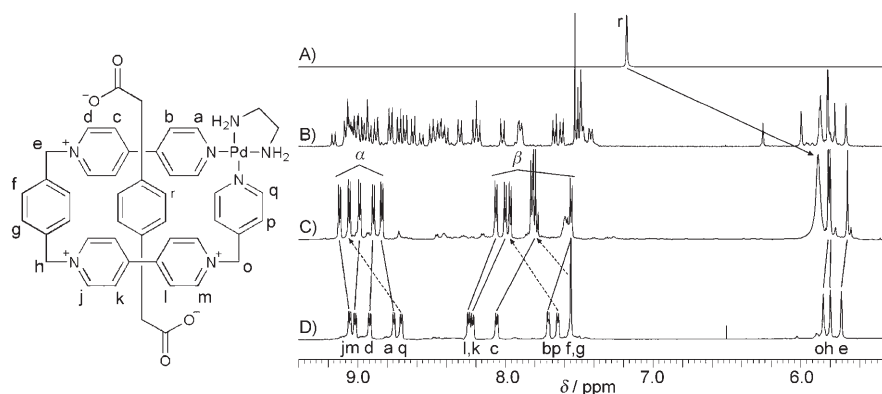

Figure 2. ^{1}H NMR (D$_2$O, 300 MHz, 298 K) spectra of: A) 12; B) a mixture of 3·3NO$_3$ (10 mM) and 6a (10 mM); C) a mixture of 3·3NO$_3$ (10 mM), 6a (10 mM), and 12 (10 mM); and D) a mixture of 3·3NO$_3$ (0.5 mM) and 6a (0.5 mM).
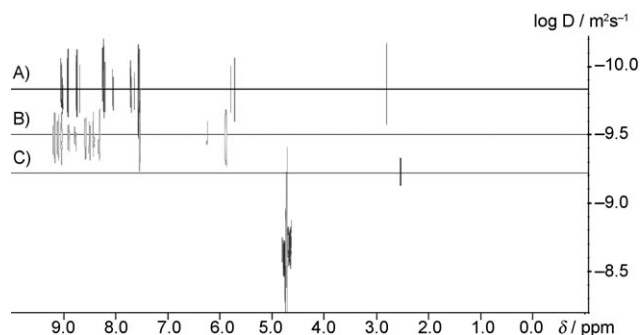
Figure 3. Superposed DOSY (D$_2$O, 500 MHz, 298 K) experiments of A) a mixture of **3**·3NO$_3$ (0.5 mM) and **6a** (0.5 mM), B) **3**·3NO$_3$, and C) **6a**.

Figure 4. ^{1}H NMR (D$_2$O, 300 MHz, 298 K) spectra of an equimolecular solution of **4**·3NO$_3$ and **6a**: A) 10 mM, B) 2 mM, C) 1 mM, and D) 0.5 mM.

Thus, the reaction between ligand **3**·3NO$_3$ and the palladium(II) complex **6a** is quite different to those of **1**·NO$_3$ and **2**·NO$_3$ with the same Pd^{II} complex. Indeed, in the first case, the formation of the desired metallocycle as a single reaction product was only achieved at relatively low concentrations. Thus, the reaction of **3**·3NO$_3$ with **6a** cannot be considered as a self-assembly process, but a simple coordination reaction. This is probably because in **9a** three sp^3 carbon atoms have to adopt an unfavorable, almost 90° angle, which probably increases the strain energy of this metallocycle with respect to that of **7a** and **7b**.

The addition of disodium *p*-phenylenediacetate (2 equiv) to an equimolecular solution of **3**·3NO$_3$ (10 mM) and **6a** (10 mM) at room temperature causes an immediate reorganization of the species present in solution to give a new species with spectral characteristics that are compatible with the inclusion of one *p*-phenylenediacetate anion in the cavity of **9a**·5NO$_3$. The ^{1}H NMR spectra for dicarboxylate **12** and **12**⊂**9a**·5NO$_3$ in D$_2$O are shown in Figure 2. The upfield shifts of the signals caused by **12** ($\Delta\delta = 1.33$ and 0.30 ppm, for H$_r$ and CH$_2$, respectively) along with the downfield shift of the protons of the rings on the short side of the rectangle (dotted arrows in Figure 2) as a result of the C−H···π interaction, strongly suggest that the template is inserted into the cavity of the metallomacrocycle. These spectral changes are similar to those observed during the formation of the analogous inclusion complex with **8a**·6NO$_3$ (see above). Thus, exploitation of the template effect can be used to obtain the metallocycle **9a**·5NO$_3$ at relatively high concentrations.

As observed for **4**·3NO$_3$, the ^{1}H NMR spectrum of a solution that results from the addition of **6a** (1 equiv) to a solution of **4**·3NO$_3$ (10 mM) results in a mixture of at least two species. Diluting this solution to 0.5 mM again simplifies the ^{1}H and ^{13}C NMR spectra so that only a single species can be detected at this concentration in solution (Figure 4). The results of mass spectrometry analysis (ESI-MS), which shows signals for various cations that result from the loss of one, two, and three nitrate anions, as well as the addition of a methanol molecule (see the Experimental Section), confirm the formation of **10a**·5NO$_3$. However, in this case, sodium *p*-phenylenediacetate does not act as a template in a self-as-
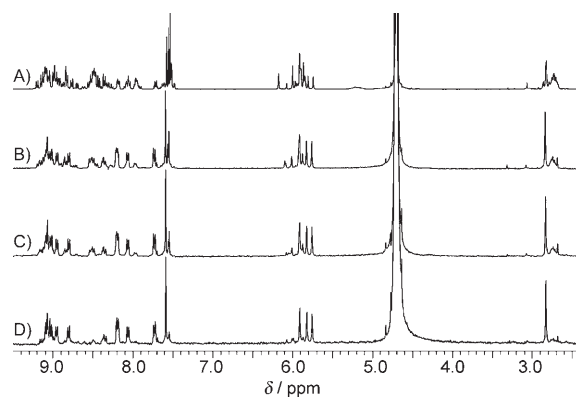
sembly process that leads to the formation of **10a**·5NO$_3$ at higher concentrations, probably as a consequence of the smaller size of the cavity of **10a**·5NO$_3$ relative to **9a**·5NO$_3$ (see below).

Notably, metallocycle **10a**·5NO$_3$ is chiral, however, the lability of the coordination bonds between the pyridine units and the palladium(II) center means that both enantiomers are in continuous interconversion.
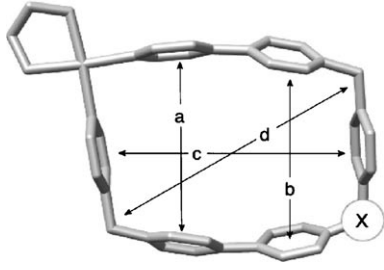
Formation of Pt^{II} metallocycles 7b·6PF$_6$, 8b·6PF$_6$, 9b·5PF$_6$, and 10b·5PF$_6$: As described in the previous sections, the lability of the coordination bonds between pyridine units and palladium(II) centers may be useful to obtain the desired structures under very mild conditions. Nevertheless, in some cases, this lability may be disadvantageous owing to the low stability of the structures obtained. The use of stronger and more inert metal–ligand bonds should stabilize the metallomacrocyclic structures and allow their isolation and a more accurate characterization. Platinum(II) metal centers, geometrically analogous to palladium(II) square-planar centers, afford much more inert coordination bonds with pyridine ligands. Furthermore, this coordination bond has double characteristics owing to its inertness at low temperature, which is lost when the temperature is increased. This dual feature was beautifully exploited by Fujita and co-workers to introduce the "molecular lock" concept.[12] The molecular lock strategy we are about to describe is similar to that originally developed by Fujita and co-workers, but with slight modifications. In our case, after the lowering the temperature, the product was precipitated as its hexafluorophosphate salt such that it was isolated from the original reaction solution.

This procedure allowed the preparation and isolation of the platinum(II) analogues of metallocycles **7–10**. The preparation procedures of all compounds were parallel to those used in the preparation of their palladium(II) analogues (i.e., strict thermodynamic self-assembly for **7b·6PF$_6$**, template-directed self-assembly for **8b·6PF$_6$** and **9b·5PF$_6$**, and high-dilution, strict thermodynamic self-assembly for **10b·5PF$_6$**) with only differences in the reaction temperature (100°C for the Pt^{II} derivatives) and the reaction time, which was increased to 12 h when the template effect was present

and up to 7 d when no template was added to the reaction mixture. All of the hexafluorophosphate salts obtained were solid products that were stable in air and light and soluble in organic solvents, such as acetonitrile or nitromethane. All of the products were unambiguously characterized by means of NMR and mass spectrometric techniques. As expected, rectangle **11b** could not be obtained by any of the self-assembly strategies described for **7b**–**10b**.

Molecular geometries of the Pt^{II} metallocycles: Metallocycles **7b**–**11b** were characterized by means of DFT calculations (B3LYP model).[13] In these calculations, the 6-31G(d) basis set was used for the ligand atoms, whereas the effective core potential of Wadt and Hay (Los Alamos ECP) included in the LanL2DZ basis set was applied to the Pt atoms.[14] The calculated structures of the platinum(II) metallocycles show a rectangular cavity with the dimensions given in Table 1.

Table 1. Cavity dimensions [Å] of the calculated structures of the platinum metallocycles.[a]

	X	a[b]	b[b]	c[c]	d[d]
7b·6PF$_6$ (*anti*)[e]	Pt(en)	2.91	2.91	8.24	7.35
7b·6PF$_6$ (*syn*)[e]	Pt(en)	2.88	2.88	8.02	7.27
8b·6PF$_6$	Pt(en)	3.92	3.92	7.07	7.61
9b·5PF$_6$	CH$_2$	4.02	3.87	6.76	7.80
10b·5PF$_6$	CH$_2$	3.32	3.62	7.17	7.61
11b·6PF$_6$	Pt(en)	3.76	3.76	7.29	7.64

[a] The dimensions were calculated by subtracting the van der Waals radii multiplied by two from the centroid–centroid or atom–atom distances. [b] Distances between the centroids defined by pyridine rings. [c] Distances between the centroids defined by the aromatic rings on the short side of the rectangle. [d] Distance between methylene groups. [e] Metallocycle **7b** can exist as two stereoisomers, the chiral C_2 (*syn*) stereoisomer, and the achiral C_s (*anti*) stereoisomer.[7]

Table 1 shows that the separation between the bipyridine moieties in most of the metallocycles is between 3.76–4.02 Å, close to the ideal value for the inclusion of an aromatic ring.[15] Thus, species with aromatic moieties could then be potential guests for our receptors.

Complexation of metallocycles 8b·6PF$_6$, 9b·5PF$_6$ and 10b·5PF$_6$ with 13: The characteristics of their central cavity and structural elements make metallocycles **7b**–**10b** potentially useful as receptors in molecular inclusion processes. This section describes the complexation process of an aromatic substrate by some of our metallocyclic receptors in an organic solvent. 1,5-Bis[2-(2-hydroxyethoxy)ethoxy]naphtha-

lene (**13**), which has two fused aromatic rings and adequate dimensions for metallocyclic cavities, was the substrate of choice. The two polyether groups at positions 1 and 5 in its aromatic system increase the electron density of **13**, which allows the formation of intense charge-transfer bands with viologen-based receptors. Moreover, additional stabilization can be achieved by C−H⋯O hydrogen bonding between the polyether oxygen atoms and the hydrogen atoms at the α or β-bipyridinium positions.[16] The hexafluorophosphate salts of **7b**–**10b** were chosen as receptors owing to their solubility in organic solvents. The cavity in **7b** is too small (2.91 Å, Table 1) to incorporate aromatic rings and no interaction with **13** was detected.

The ^{1}H NMR spectrum of an equimolar solution of **8b**·6PF$_6$ (5 mM) and **13** (5 mM) in CD$_3$NO$_2$ shows broad signals, which indicates an equilibrium situation that is close to coalescence (Figure 5B). When the temperature was low-
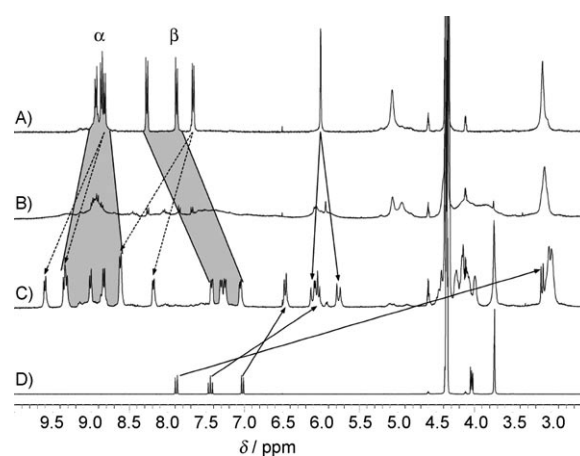

Figure 5. ^{1}H NMR (CD$_3$NO$_2$, 300 MHz) spectra of A) **8b**·6PF$_6$; B) a mixture of **8b**·6PF$_6$ (5.0 mM) and **13** (5.0 mM), 298 K; C) a mixture of **8b**·6PF$_6$ (5 mM) and **13** (5 mM), 250 K; and D) **13**.

ered to 250 K, the spectrum showed well-resolved signals. At this temperature, two sets of signals were observed for the proton nuclei of the metallocycle, whereas the signals for the aromatic protons of **13** show very important upfield shifts (Figure 5). The explanation for the observation of two sets of signals in the ^{1}H NMR spectrum can be found by looking at the symmetry of the inclusion complex. The inclusion of the naphthalene moiety inside the cavity lowers the symmetry of the receptor from C_{2h} in **8b**·6PF$_6$ to C_i in **13**⊂**8b**·6PF$_6$ (Figure 6A). Moreover, the presence of the guest precludes the free rotation of the metallocycle aromatic rings.

The symmetry of the complex implies the presence of only three signals (two doublets and one singlet) for the proton nuclei of the naphthalene ring. As expected, the doublet that corresponds to the protons involved in the C−H⋯π interaction with the perpendicular pyridine ring in the short side of the rectangle shifts upfield by $\Delta\delta = \approx 5$ ppm upon the formation of the inclusion complex. On the contrary, the signals for these pyridine rings are shifted downfield (dotted
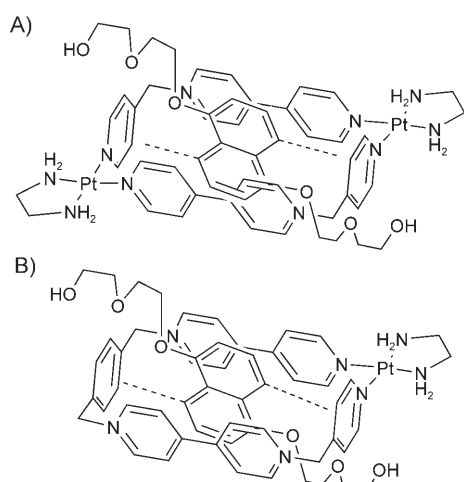
Figure 6. Structures of A) $13 \subset 8b \cdot 6 PF_6$ and B) $13 \subset 9b \cdot 6 PF_6$ showing the C−H···π interactions.

arrows in Figure 5). The naphthalenic protons involved in the C−H···π interactions for this type of inclusion complex are the ones in the 4 and 8 positions. This is attributed to the fact that it is impossible for the other protons of the naphthalenic unit to interact with the pyridine ring. We have observed that the naphthalene group does not fit into the cavity of related metallocycles with any other pair of protons oriented towards the accepting pyridine rings.[17]

A solution of equimolar amounts of **13** and **9b**·5 PF₆ in nitromethane is red; however, in this case, the coloration is much more intense than for **8b**·6 PF₆. This suggests a rather strong interaction between **9b**·5 PF₆ and **13** in nitromethane (see below). The ¹H NMR spectrum of the mixture showed, as in the previous case, broad signals that indicated an equilibrium situation in solution that was close to coalescence (Figure 7B). When the sample was cooled to 250 K, the signals were well-defined so that the spectral changes that ori-
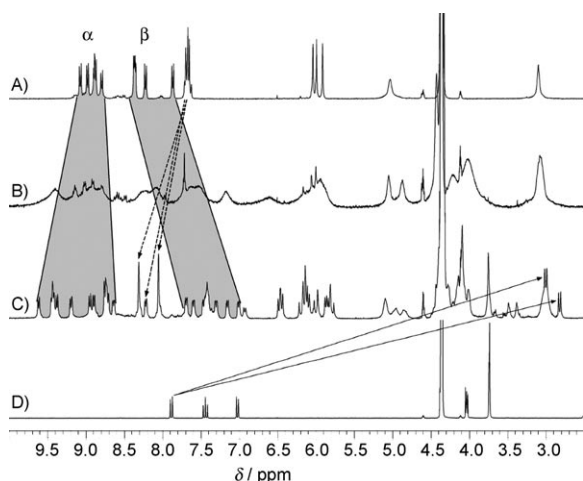

Figure 7. ¹H NMR (CD₃NO₂, 300 MHz) spectra of: A) **9b**·5 PF₆; B) a mixture of **9b**·6 PF₆ (5.0 mM) and **13** (5.0 mM), 298 ; C) a mixture of **9b**·6 PF₆ (5 mM) and **13** (5 mM), 250 ; and D) **13**.

ginated from the formation of the supramolecular complex could be interpreted. As observed in the previous example, each of the ¹H NMR signals of **9b**·5 PF₆ splits into two upon the formation of the inclusion complex. Moreover, the same signal splitting is observed for the resonances of the naphthalene moiety; this is because the inclusion of **13** inside the cavity lowers the symmetry of the receptor from C_s symmetry in **9b**·6 PF₆ to C_1 in $13 \subset 9b \cdot 6 PF_6$ (Figure 6B). The nonequivalent protons, now in the 4 and 8 positions of the naphthalene moiety, interact by means of C−H···π bonds with the short sides of the metallocycle (Figure 6B), as demonstrated by the pronounced upfield shifts of their signals (continuous arrows in Figure 7) of up to $\Delta\delta = 5$ ppm. The reverse downfield shifts of the acceptor aromatic ring proton signals (dotted arrows in Figure 7) was also evidence for this interaction. Another consequence of the C_1 symmetry of the inclusion complex is that two different isomers may exist in solution that depend on the position of the guest in the cavity. These isomers are enantiomers and their existence is consistent with the observed ¹H NMR spectrum.

In a static situation, metallocycle **10b**·5 PF₆ belongs to the C_1 point group, and therefore, it is obtained as a racemic mixture of the two possible enantiomers. Nevertheless, its ¹H NMR spectrum shows only eight doublets associated with the bipyridinium protons (Figure 8); this is attributed
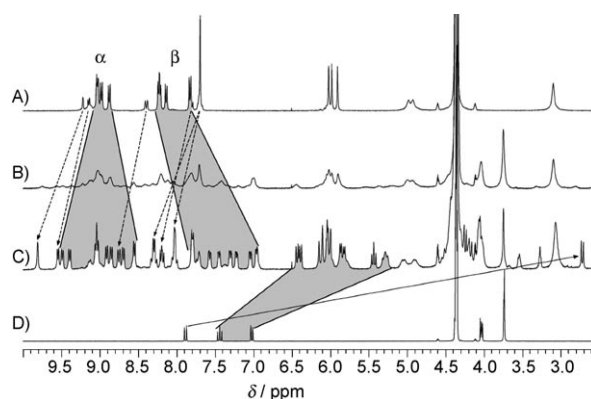
Figure 8. ¹H NMR (CD₃NO₂, 300 MHz) spectra of: A) **10b**·5 PF₆; B) a mixture of **10b**·6 PF₆ (5.0 mM) and **13** (5.0 mM), 298 K; C) a mixture of **10b**·6 PF₆ (5 mM) and **13** (5 mM), 250 K; and D) **13**.

to the fast rotation of the phenylene and bipyridine aromatic rings on the NMR timescale. After addition of **13** (1 equiv), the ¹H NMR spectrum shows broad bands, as in the previous examples (Figure 8B). After cooling the sample to 250 K, the spectrum shows well-defined signals (Figure 8C). From observation of the low-temperature ¹H NMR spectrum, information on the system could be obtained:

a) All of the signals show the expected shifts after the inclusion of **13** in the metallocycle cavity; the aromatic signals of **13** are shifted upfield, especially those involved in the C−H···π interactions, which are shifted by more than 5 ppm (continuous arrows in Figure 8). Moreover, the

signals from the acceptor aromatic rings involved in these interactions are shifted downfield owing to de-shielding caused by the ring currents of **13** (dotted arrows in Figure 8).

b) All of the proton nuclei of the metallocycle are nonequivalent. However, the inclusion of **13** in the cavity does not imply any change in the symmetry of the system in this case; however, the fact that rotation of the metallocycle aromatic rings upon formation of the inclusion complex is impossible causes the signals of **10b·5PF$_6$** to split in two groups.

c) A careful study of the geometry of the inclusion complex **13⊂10b·5PF$_6$** indicated that two different species could be formed, which depended on the diol orientation inside the cavity of the two enantiomers. However, this is not observed in the NMR spectrum, except for a slight splitting of the signals from the bipyridine β protons.

Complexation of metallocycle 11a·6NO$_3$ with hydroquinone (HQ) and 13, and the crystal structure: As mentioned above, metallocycle **11a·6NO$_3$** could not be self-assembled in solution by any of the self-assembly methods attempted. However, single crystals that were suitable for X-ray crystallography were grown from a solution of **5·NO$_3$**/[Pd(en)-(NO$_3$)$_2$]/HQ (2:2:1 molar ratio) in 3 M aqueous NaNO$_3$. The solid-state structure shows a molecule of hydroquinone inserted inside the cavity of the dipalladium metallocycle (Figure 9). The metal cent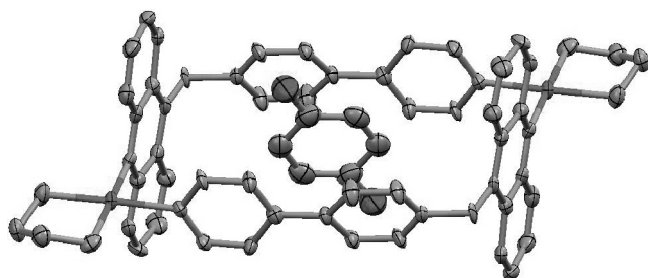ers show a square-planar geometry in which the bond lengths and angles are in the normal range, Pd−N(Py) 2.05 Å, N(Py)-Pd-N(Py) 87.7°. The dimensions of the rectangle are 10.45 × 6.97 Å. The acridine aromatic systems are almost perpendicular (89°) to the metallocycle mean plane defined by the palladium atoms and the methylene groups. The distance between the centroid of the central C−C bond of the bipyridines and the centroid of the hydroquinone ring is 3.49 Å. As a result of a C−H···π interaction, the distance between the centroid of one acridine spacer and the closest CH group of the hydroquinone is 3.07 Å, whereas the angle defined by these three positions amounts to 157°.

The ^{1}H NMR spectrum of a solution of these crystals in D$_2$O revealed that the 1:1 inclusion complex was maintained

in solution. At room temperature, the complexation process was fast and led to an averaging of the ^{1}H NMR signals of the hydroquinone that was inside/outside of the metallocycle cavity ($\delta = 5.08$ ppm). After addition of cerium ammonium nitrate (CAN, 1.5 equiv), the signal at $\delta = 5.08$ ppm disappeared and a new resonance for benzoquinone was detected at $\delta = 6.86$ ppm as a result of the oxidation of the hydroquinone. This chemical shift indicates that there is no interaction between **11a·6NO$_3$** and benzoquinone in D$_2$O. Upon addition of NaBH$_4$ (1.5 equiv), benzoquinone was reduced and the inclusion complex with hydroquinone was formed again (see the Supporting Information). The overall process involved the chemically controlled formation of the inclusion complex with hydroquinone.

In the same manner, single crystals that were suitable for X-ray crystallography were obtained from a solution of **5·NO$_3$**/[Pd(en)(NO$_3$)$_2$]/**13** in 3 M aqueous NaNO$_3$. The crystal structure shows the insertion of **13** into the cavity of **11a·6NO$_3$** (Figure 10). In addition to π–π stacking interac-
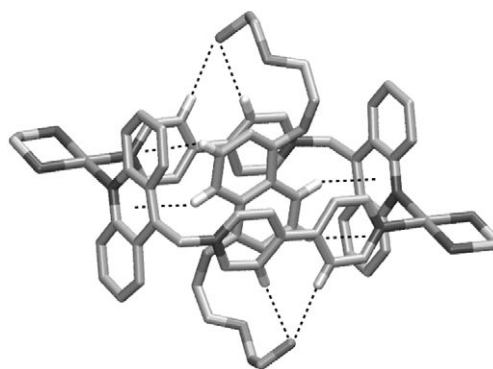

Figure 9. Crystal structure of HQ⊂**11a·6NO$_3$**. Solvent molecules, counterions, and hydrogen atoms have been omitted for clarity.

Figure 10. Crystal structure of **13⊂11a·6NO$_3$**, which shows the two pairs of bifurcated C−H···O hydrogen bonds and the four C−H···π interactions. The second molecule of **13**, solvent molecules, counterions, and hydrogen atoms have been omitted for clarity.

tions, the complex is stabilized by two pairs of bifurcated C−H···O hydrogen bonds between two of the β-CH bipyridinium hydrogen atoms and the free hydroxyl group.[18] There are also four C−H···π interactions between hydrogen atoms H4 and H8 of the guest with the central aromatic ring of the acridine system (H···π distances: 2.65 Å and 2.80 Å, angles: 152° and 145°) and between H3 and H7 with one of the lateral rings of the acridine system (H···π distances: 2.65 Å and 2.68 Å, angles: 156° and 153°). Inspection of the crystal structure of the complex revealed a second molecule of **13** that sustains hydrogen-bonding interactions with one of the free hydroxyl groups of the naphthalene moiety inside the metallocycle. The inclusion complex was studied in solution after redissolution in D$_2$O. The ^{1}H NMR spectrum of **13⊂11a·6NO$_3$** confirmed the existence of the inclusion complex in D$_2$O (Figure 11). In this case, at room temperature, the equilibrium is slow on the ^{1}H NMR timescale and well-defined signals are observed, probably owing to the excel-
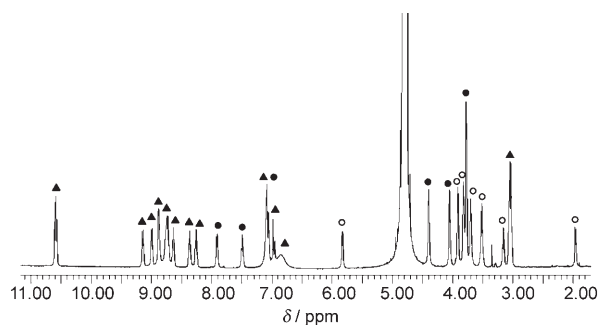
Figure 11. ^{1}H NMR (D$_2$O, 500 MHz) spectrum of **13**⊂**11 a**·6 NO$_3$ obtained upon redissolution in D$_2$O of the crystals. Signals that correspond to **11 a** (▲), bound **13** (○), and free **13** (●) have been indicated on the spectrum.

lent fit of **13** to metallocycle **11 a**. Thus, protons H4/H8 and H3/H7 of diol **13**, which are involved in C−H···π interactions, are shifted upfield ($\Delta\delta = 5.97$ ppm and $\Delta\delta = 4.35$ ppm, respectively). Moreover, the introduction of the 1,5-naphthalene unit into the metallocycle results in the inequivalence of the eight bipyridine protons and the eight acridine protons. The signals associated with the second equivalent of **13** are detected at the chemical shifts expected if there is no interaction with **11 b**.

Determination of binding constants: As previously mentioned, the inclusion of **13** in the cavity of the different metallocycles presented in this work results in the appearance of a reddish color of differing intensity that originates from charge-transfer bands between the electron-rich substrate and the receptor in the inclusion complex. This kind of interaction usually makes a very small contribution to the stability of the complex; however, these charge-transfer bands are very useful for the determination of the association constant by means of UV-visible spectroscopy.[19]

Indeed, we used UV-visible spectroscopy to determine the association constants for ten different systems. The interactions between receptors **8 b**·6 PF$_6$, **9 b**·5 PF$_6$, and **10 b**·5 PF$_6$ and substrate **13** were studied in nitromethane. The nitrate salts of the same receptors were also used to study their interaction with diol 1,4-bis[2-(2-hydroxyethoxy)ethoxy]benzene (**14**) in water. The binding of palladium(II) analogues **8 a**·6 NO$_3$, **9 a**·5 NO$_3$, and **10 a**·5 NO$_3$ with **14** in aqueous solution was also studied. The charge-transfer bands caused by the binding of **14** are less intense and the association constants were lower than those observed for **13**, but the solubility of **14** in water is much higher. The values of the binding constants obtained from these studies (Table 2) are consistent with the ^{1}H NMR studies and DFT calculations described above. A comparison of the binding data obtained for these metallocycles (Table 2) with the geometrical parameters predicted by our DFT calculations allows us to draw some conclusions on their properties as receptors:

a) Metallocycle **9** and, to a lesser extent, **8** are the receptors with the greatest affinity for the substrates under all conditions, which reflects the fact that the sizes of their cavi-

Table 2. Equilibrium association constants [L mol^{-1}] and standard free energies [kcal mol^{-1}] for the formation the of 1:1 inclusion complex[a] between substrates **13**–**14** and the metallocycles **8**–**10** at 26 °C.[b]

	K		$-\Delta G°$	Substrate
	CH$_3$NO$_2$	H$_2$O		
8 b·6 PF$_6$	1180±30		4.2	**13**
9 b·5 PF$_6$	$1.3 \times 10^4 \pm 2 \times 10^3$		5.6	**13**
10 b·5 PF$_6$	197±4		3.1	**13**
8 b·6 NO$_3$		248±3	3.3	**14**
9 b·5 NO$_3$		1670±30	4.4	**14**
10 b·5 NO$_3$		nb[c]	–	**14**
8 a·6 NO$_3$		212±3	3.2	**14**
9 a·5 NO$_3$		1330±11	4.3	**14**
10 a·5 NO$_3$		123±4	2.9	**14**

[a] Job's plots showed that maximum complexation occurred at 0.5 molar fraction of receptor. [b] Metallocycle concentrations: **8 b**–**10 b** 1×10^{-3} M, **8 a**–**10 a** 5×10^{-4} M. [c] No binding detected.

ties match the ideal separation for π–π stacking (Table 1).

b) On the other hand, macrocycles **10 a,b** are worse receptors than **9** and **8** such that no complexation between **10 b** and **14** was detected in water. Finally, no binding was detected for metallocycles **7 a,b**. This can be explained by the short distance between bipyridine systems in these metallocycles.

c) The equilibrium association constants in water for the formation of the complexes between **14** and **8 a**–**10 a** are very similar to those in **8 b**–**10 b**, which reflects the similarity of their cavity sizes.

Conclusion

In summary, we have enlarged the structural diversity of mononuclear and dinuclear Pd^{II} and Pt^{II} rectangular metallocycles with a well-defined internal cavity. Metallocycles **7 a,b** were synthesized by strict thermodynamic self-assembly, **8 a,b** and **9 a,b** required a templated self-assembly process, and finally, metallocycles **10 a,b** were synthesized under high dilution conditions. The inclusion complexes of these metallocycles with aromatic guests, such as **12**–**14**, were studied by NMR techniques that indicate the insertion of the guests into the cavity of the metallocycle and C−H···π interactions between guest protons and the pyridine or *p*-phenylene rings on the short side of the rectangle. This disposition was also found in the solid state, as revealed by X-ray diffraction analysis of the inclusion complexes of **11 a**·4 NO$_3$ with hydroquinone and with **13**.

The association constants measured by UV-visible spectroscopy show a clear correlation between the stability of the inclusion complex and the size of the cavity determined by DFT calculations. Thus, metallocycles **8 b** and **9 b** exhibit the highest binding constants in both nitromethane and water owing to the ideal dimensions of their cavity.

Experimental Section

Materials: Ligands **1–3** and metallocycles **7–9 a,b** were prepared by the methods described in our previous reports.[8] Substrates **13**,[20] and **14**[21] were prepared according to published procedures.

General: All of the other reagents were of analytical grade and were used as received. Milli-Q water was purified with a Millipore Gradient A10 apparatus. Merck 60 HF$_{254+366}$ foils were used for thin-layer chromatography and Merck 60 (230–400 mesh) silica gel was used for flash chromatography. NMR spectra were obtained by using a Bruker Avance 500 spectrometer equipped with a dual cryoprobe for ^{1}H and ^{13}C and a Bruker Avance 300 spectrometer (for low- and high-temperature experiments). TMS was used as an internal reference. Diffusion coefficients from DOSY experiments were referenced by using a value of 1.92× 10^{-9} m^{2}s for the DHO signal in D$_2$O at 298 K.[22] Mass spectrometry experiments were carried out with a Fision VG-Quattro spectrometer for low-resolution FAB with 3-NBA as the matrix, a VG Autospec M spectrometer for high-resolution FAB with 3-NBA as the matrix, a Navigator spectrometer for low-resolution ES with MeOH and CH$_3$CN as the solvents, and a Bruker BioTOF II for high-resolution ES with CH$_3$NO$_2$ as the solvent. UV-visible spectra were recorded by using a Perkin–Elmer Lambda 900 spectrometer. Melting points were measured by using a Stuart Scientific SMP3 instrument.

Ligand 4·3 PF$_6$: A solution of NaOH (0.474 g, 11.9 mmol) in water (5 mL) was added to a solution of 3-(bromomethyl)pyridine hydrobromide (3.0 g, 11.9 mmol) in water (60 mL). The solution was extracted with nitromethane (2×60 mL). The combined organic layers were added to a solution of 1,1′-[1,4-phenylenebis(phenylen)]bis-4,4′-bipyridine bis(hexafluorophosphate) (5.98 g, 8.5 mmol) in nitromethane (20 mL) at reflux. Heating was continued for 18 h. After the solution had cooled, the solvent was removed in vacuo to leave a solid residue that was subjected to flash column chromatography (SiO$_2$, acetone/MeOH/NH$_4$Cl(aq, 1.5 M), 5:1:4). The ligand-containing fractions were combined and the solvents were removed in vacuo. The residue was dissolved in H$_2$O (100 mL), and a saturated aqueous solution of NH$_4$PF$_6$ was added until no further precipitation was observed. This mixture was extracted with nitromethane (3×100 mL). The combined organic layers were dried (MgSO$_4$) and evaporated in vacuo. The residue was triturated in H$_2$O and filtered to yield **4**·3 PF$_6$ (1.46 g, 19%). M.p. 178–180 °C (decomp); ^{1}H NMR (500 MHz, CD$_3$NO$_2$, 25 °C): δ = 6.00 (s, 2H), 6.02 (s, 2H), 6.16 (s, 2H), 7.68 (s, 4H), 7.88 (dd, J(H,H) = 8.2, 5.5 Hz, 1H), 8.24 (d, J-(H,H) = 6.4 Hz, 2H), 8.34–8.38 (m, 1H), 8.51 (d, J(H,H) = 6.4 Hz, 2H), 8.53 (d, J(H,H) = 6.4 Hz, 2H), 8.56 (d, J(H,H) = 6.4 Hz, 2H), 8.82–8.86 (m, 1H), 8.90–8.94 (m, 1H), 8.99 (d, J(H,H) = 6.4 Hz, 2H), 9.04 (d, J-(H,H) = 6.4 Hz, 2H), 9.10 (d, J(H,H) = 6.4 Hz, 2H), 9.14 (d, J(H,H) = 6.4 Hz, 2H); ^{13}C NMR (125 MHz, CD$_3$NO$_2$, 25 °C): δ = 61.9 (CH$_2$), 64.2 (CH$_2$), 64.6 (CH$_2$), 124.4 (CH), 126.4 (CH), 127.0 (CH), 127.6 (CH), 127.8 (CH), 130.4 (CH), 130.5 (CH), 134.1, 134.5, 142.4 (CH), 145.2 (CH), 145.6 (CH), 145.8 (CH), 146.4 (CH), 146.7 (CH), 147.3, 147.6 (CH), 150.8, 151.4, 153.2; MS (ES): m/z: 798.2 [M−PF$_6$]$^+$, 652.3 [M−2 PF$_6$−H]$^+$, 506.2 [M−3 PF$_6$−2 H]$^+$.

Ligand 4·3 NO$_3$: A mixture of **4**·3 PF$_6$ (1.15 g, 1.22 mmol) and Amberlite CG-400 (5.0 g) in H$_2$O (50 mL) was stirred for 4 h. The resin was removed by filtration and the filtrate evaporated to give **4**·3 Cl (0.75 g, quantitative). A solution of **4**·3 Cl (0.75 g, 1.22 mmol) and AgNO$_3$ (0.621 g, 3.66 mmol) in H$_2$O (50 mL) was stirred at room temperature for 3 h. The mixture was filtered and the filtrate was evaporated in vacuo to give **4**·3 NO$_3$ (0.85 g, quantitative). M.p. 160–162 °C; ^{1}H NMR (500 MHz, CD$_3$NO$_2$, 25 °C): δ = 5.94 (s, 2H), 5.97 (s, 2H), 6.11 (s, 2H), 7.60 (s, 4H), 7.80–7.85 (m, 1H), 8.23 (d, J(H,H) = 5.5 Hz, 2H), 8.28–8.33 (m, 1H), 8.47 (d, J(H,H) = 6.9 Hz, 2H), 8.54 (d, J(H,H) = 6.9 Hz, 2H), 8.57 (d, J-(H,H) = 6.9 Hz, 2H), 8.73–8.77 (m, 1H), 8.86 (br s, 1H), 8.90 (d, J-(H,H) = 5.5 Hz, 2H), 9.08 (d, J(H,H) = 6.9 Hz, 2H), 9.15 (d, J(H,H) = 6.9 Hz, 2H), 9.22 (d, J(H,H) = 6.9 Hz, 2H); ^{13}C NMR (125 MHz, D$_2$O, 25 °C): δ = 61.3 (CH$_2$), 63.8 (CH$_2$), 64.2 (CH$_2$), 124.6 (CH), 126.4 (CH), 126.8 (CH), 127.2 (CH), 127.4 (CH), 130.1 (CH), 130.2 (CH), 130.5, 133.9, 134.3, 142.2 (CH), 145.3 (CH), 145.6 (CH), 145.8 (CH), 145.9 (CH), 145.9 (CH), 146.9 (CH), 147.4, 150.2, 150.9, 152.6; MS (ES): m/z:

632.2 [M−NO$_3$]$^+$, 570.4 [M−2 NO$_3$]$^+$, 508.4 [M−3 NO$_3$]$^+$; elemental analysis calcd (%) for C$_{34}$H$_{30}$N$_8$O$_9$: C 58.79, H 4.35, N 16.13; found: C 58.92, H 4.28, N 16.19.

Ligand 5·PF$_6$: A solution of 4,4′-bipyridine (0.57 g, 3.68 mmol) and 9-bromomethylacridine (0.2 g, 0.74 mmol) in nitromethane (20 mL) was heated at reflux for 24 h. After cooling, the solvent was evaporated under reduced pressure and the residue was triturated in Et$_2$O. The solid obtained was purified by flash column chromatography (SiO$_2$, acetone/MeOH/NH$_4$Cl (aq, 1.5 M), 5:1:4). The ligand-containing fractions were combined and the solvents were removed in vacuo. The residue was dissolved in H$_2$O (100 mL) and a saturated aqueous solution of NH$_4$PF$_6$ was added until no further precipitation was observed. The solid was filtered and washed with water to give **5**·PF$_6$ (0.36 g, 25%). M.p. 167–168 °C; ^{1}H NMR (300 MHz, CD$_3$NO$_2$, 25 °C): δ = 7.25 (s, 2H), 8.03–8.10 (m, 2H), 8.26 (d, J(H,H) = 6.6 Hz, 2H), 8.30–8.37 (m, 2H), 8.48 (d, J(H,H) = 6.8 Hz, 2H), 8.55 (d, J(H,H) = 8.9 Hz, 2H), 8.65 (d, J(H,H) = 8.9 Hz, 2H), 9.00 (d, J(H,H) = 6.6 Hz, 2H), 9.04 (d, J(H,H) = 6.8 Hz, 2H); elemental analysis calcd (%) for C$_{24}$H$_{18}$F$_6$N$_3$P: C 58.42, H 3.68, N 8.52; found: C 58.69, H 3.42, N 8.41.

Ligand 5·NO$_3$: This compound was obtained from **5**·PF$_6$ by following the described procedure for **4**·3 NO$_3$ (98%). M.p. 167–168 °C; ^{1}H NMR (500 MHz, D$_2$O, 25 °C): δ = 8.07–8.10 (m, 2H), 8.34–8.39 (m, 2H), 8.40 (d, J(H,H) = 6.5 Hz, 2H), 8.49 (d, J(H,H) = 8.8 Hz, 2H), 8.54 (d, J-(H,H) = 7.0 Hz, 2H), 8.66 (d, J(H,H) = 8.9 Hz, 2H), 9.01 (d, J(H,H) = 6.5 Hz, 2H), 9.09 (d, J(H,H) = 7.0 Hz, 2H); ^{13}C NMR (125 MHz, D$_2$O, 25 °C): δ = 152.6, 149.0, 145.2 (CH), 144.3 (CH), 142.6, 141.0, 137.0 (CH), 130.2 (CH), 127.4 (CH), 126.3, 125.5 (CH), 124.2 (CH), 122.0 (CH); MS (FAB): m/z: 348 [M−NO$_3$]$^+$; elemental analysis calcd (%) for C$_{24}$H$_{18}$N$_4$O$_3$: C 70.23, H 4.42, N 13.65; found: C 70.48, H 4.20, N 13.32.

Metallocycle 10 a·5 NO$_3$: Complex **6 a** (1.7 mg, 6.0×10^{-3} mmol) was added to a solution of **4**·NO$_3$ (4.2 mg, 6.0×10^{-3} mmol) in D$_2$O (12 mL). (The compound was not isolated; data are taken from measurements on the reaction mixture.) ^{1}H NMR (500 MHz, D$_2$O, 25 °C): δ = 2.87 (s, 4H), 5.80 (s, 2H), 5.86 (s, 2H), 5.95 (s, 2H) , 7.63 (s, 4H), 7.74–7.80 (m, 3H), 8.10 (d, J(H,H) = 6.9 Hz, 2H), 8.21–8.26 (m, 4H), 8.38–8.42 (m, 1H), 8.84 (d, J(H,H) = 6.7 Hz, 2H), 9.00 (d, J(H,H) = 6.9 Hz, 2H), 9.05–9.14 (m, 6H); ^{13}C NMR (125 MHz, D$_2$O, 25 °C): δ = 46.7 (CH$_2$), 46.8 (CH$_2$), 61.2 (CH$_2$), 64.7 (CH$_2$), 65.1 (CH$_2$), 124.7 (CH), 126.6 (CH), 127.2 (CH), 127.4 (CH), 127.7 (CH), 130.0 (CH), 130.1 (CH), 131.9, 136.2, 136.3, 142.7 (CH), 144.3 (CH), 144.7 (CH), 144.89 (CH), 144.84, 149.6, 150.2, 151.3, 151.9 (CH), 152.3, 152.9; MS (ES): m/z: 445.2 [M−2 NO$_3$+CH$_3$OH]$^{2+}$, 413.8 [M−3 NO$_3$−H+CH$_3$OH]$^{2+}$, 384.5 [M−4 NO$_3$−2 H+CH$_3$OH]$^{2+}$.

Metallocycle 10 b·5 PF$_6$: A solution of ligand **4**·NO$_3$ (34.1 mg, 0.049 mmol) and complex **6 b** (18.5 mg, 0.049 mmol) in H$_2$O (100 mL) was heated at 100 °C for 7 d. After cooling to room temperature, NH$_4$PF$_6$ (3.00 g, 18.6 mmol) was added and a white solid precipitated. The precipitate was filtered and washed with H$_2$O to afford metallocycle **10 b**·5 PF$_6$ (43.4 mg, 59%). M.p. 206–208 °C (decomp); ^{1}H NMR (500 MHz, CD$_3$NO$_2$, 25 °C): δ = 3.06 (br s, 4H), 4.90 (br s, 2H), 4.96 (br s, 2H), 5.88 (s, 2H), 5.95 (s, 2H), 5.99 (s, 2H), 7.64–7.69 (m, 4H), 7.76–7.81 (m, 4H), 8.10 (d, J(H,H) = 7.33 Hz, 2H), 8.17–8.22 (m, 4H), 8.35–8.38 (m, 1H), 8.85 (d, J(H,H) = 7.33 Hz, 2H), 8.95 (d, J(H,H) = 6.9 Hz, 2H), 8.98–9.02 (m, 4H), 9.10–9.13 (m, 1H), 9.19 (br s, 1H); ^{13}C NMR (125 MHz, CD$_3$NO$_2$, 25 °C): δ = 48.23 (CH$_2$), 48.25 (CH$_2$), 61.5 (CH$_2$), 65.2 (CH$_2$), 65.8 (CH$_2$), 125.3 (CH), 126.6 (CH), 127.6 (CH), 127.7 (CH),128.6 (CH), 130.2 (CH), 130.6 (CH), 132.3, 136.3, 136.6, 142.8 (CH), 144.5 (CH), 144.7 (CH), 144.9 (CH), 145.1, 150.2, 151.1, 151.6, 152.6 (CH), 153.3 (CH), 154.5 (CH) ; MS (ES): m/z: 1197.2 [M−2 PF$_6$−H]$^+$, 1051.2 [M−3 PF$_6$−2 H]$^+$, 526.1 [M−3 PF$_6$−H]$^{2+}$; elemental analysis calcd (%) for C$_{36}$H$_{38}$F$_{30}$N$_7$P$_5$Pt: C 29.05, H 2.57, N 6.59; found: C 28.79, H 2.70, N 6.69.

Crystal structure analysis: CCDC-641682 and CCDC-643799 contain the supplementary crystallographic data for HQ⊂**11 a**·6 NO$_3$ and **13**⊂**11 a**·6 NO$_3$, respectively. These data can be obtained free of charge from the Cambridge Crystallographic Data Centre via www.ccdc.cam. ac.uk/data_request/cif. Crystal data are reported in Table 3. The structure was solved by direct methods and refined with the full-matrix least-squares procedure (SHELXTL[23]) against F^2. The X-ray diffraction data

Table 3. Summary of the crystal data, intensity measurements, and structure refinement.

	HQ⊂11a·6NO₃	13⊂11a·6NO₃
formula	$C_{58}H_{74}N_{16}O_{30}Pd_2$	$C_{88}H_{100}N_{16}O_{34}Pd_2$
M_W	1688.13	2138.64
λ [Å]	0.71073	0.71073
crystal size [mm³]	$0.43 \times 0.26 \times 0.04$	$0.25 \times 0.06 \times 0.03$
crystal system	triclinic	triclinic
space group	$P\bar{1}$	$P\bar{1}$
a [Å]	9.464(3)	12.055(5)
b [Å]	13.923(3)	13.560(5)
c [Å]	14.296(4)	14.250(5)
α [°]	94.847(4)	81.261(5)
β [°]	108.088(3)	81.087(5)
γ [°]	100.099(2)	84.969(5)
V [Å³]	1743.4(8)	2269.6(15)
Z	1	2
ρ_{calcd} [mgm⁻³]	1.608	1.565
μ [mm⁻¹]	0.615	0.494
θ range [°]	1.52–25.21	1.46–28.42
index range	$-10 \leq h \leq 10$	$-16 \leq h \leq 16$
	$-13 \leq k \leq 16$	$-17 \leq k \leq 18$
	$-17 \leq l \leq 17$	$-19 \leq l \leq 19$
T [K]	100(2)	100(2)
independent reflns	5561	11263
R_{int}	0.0353	0.1069
refinement method	based on F^2	based on F^2
final R indices [$I > 2\sigma(I)$]	$R_1 = 0.0823$	$R_1 = 0.0592$
	$wR_2 = 0.2252$	$wR_2 = 0.1223$
R indices (all data)	$R_1 = 0.1142$	$R_1 = 0.1028$
	$wR_2 = 0.2591$	$wR_2 = 0.1431$

were collected on a Bruker SMART APEX CCD diffractometer. Hydrogen atoms were placed in idealized positions with $U_{eg}(H) = 1.2\,U_{eg}(C)$ and were allowed to ride on their parent atoms.

Acknowledgements

[1] a) G. F. Swiegers, T. J. Malefetse, *Chem. Rev.* **2000**, *100*, 3483–3537; b) M. Fujita, M. Tominaga, A. Hori, B. Therrien, *Acc. Chem. Res.* **2005**, *38*, 369–378; c) P. H. Dinolfo, J. T. Hupp, *Chem. Mater.* **2001**, *13*, 3113–3125; d) D. L. Caulder, K. N. Raymond, *J. Chem. Soc. Dalton Trans.* **1999**, 1185–1200; e) P. J. Steel, *Acc. Chem. Res.* **2005**, *38*, 243–250; f) M. Fujita, *Chem. Soc. Rev.* **1998**, *27*, 417–425; g) S. Leininger, B. Olenyuk, P. J. Stang, *Chem. Rev.* **2000**, *100*, 853–908; h) B. Holliday, C. A. Mirkin, *Angew. Chem.* **2001**, *113*, 2076–2097; *Angew. Chem. Int. Ed.* **2001**, *40*, 2022–2043; i) F. Würthner, C.-C. You, C. R. Saha-Möller *Chem. Soc. Rev.* **2004**, 133–146; j) J.-P. Collin, V. Heitz, S. Bonnet, J.-P. Sauvage, *Inorg. Chem. Commun.* **2005**, *1*, 1063–1074.

[2] a) J.-P. Sauvage, *Chem. Commun.* **2005**, 1507–1510; b) L. Raehm, J.-P. Sauvage in *Molecular Machines and Motors: Structure and Bonding* (Ed.: J.-P. Sauvage), Springer, Berlin, **2001**, pp. 55–78; c) O. Ohmori, M. Fujita, *Chem. Commun.* **2004**, 1586–1587; d) S.-S. Sun, A. J. Lees, *Inorg. Chem.* **2001**, *40*, 3154–3160; e) S.-S. Sun, A. J. Lees, *Coord. Chem. Rev.* **2002**, *230*, 171–192; f) K. Biradha, M.

Fujita, *Chem. Commun.* **2001**, 15–16; g) S. J. Lee, W. Lin, *J. Am. Chem. Soc.* **2002**, *124*, 4554–4555; h) M. J. E. Resendiz, J. C. Noveron, H. Disteldorf, S. Fischer, P. J. Stang, *Org. Lett.* **2004**, *6*, 651–653; i) M. L. Merlau, M. del Pilar Mejia, S. T. Nguyen, J. T. Hupp, *Angew. Chem.* **2001**, *113*, 4369–4372; *Angew. Chem. Int. Ed.* **2001**, *40*, 4239–4242; j) N. L. S. Yue, M. C. Jennings, R. J. Puddephatt, *Inorg. Chem.* **2005**, *44*, 1125–1131; A. V. Davis, K. N. Raymond, *J. Am. Chem. Soc.* **2005**, *127*, 7912–7919.

[3] a) G. Tárkányi, H. Jude, G. Pálinkás, P. J. Stang, *Org. Lett.* **2005**, *7*, 4971–4973; b) D. E. Janzen, K. N. Patel, D. G. VanDerveer, G. J. Grant, *Chem. Commun.* **2006**, 3540–3542; c) Z.-Q. Wu, X.-K. Jiang, Z.-T. Li, *Tetrahedron Lett.* **2005**, *46*, 8067–8070; d) C. S. Campos-Fernández, B. L. Schottel, H. T. Chifotides, J. K. Bera, J. Bacsa, J. M. Koomen, D. H. Russell, K. R. Dunbar, *J. Am. Chem. Soc.* **2005**, *127*, 12909–12923; e) H. Jiang, W. Lin, *J. Am. Chem. Soc.* **2003**, *125*, 8084–8085; f) Y. L. Cho, H. Uh, S.-Y. Chang, H.-Y. Chang, M.-G. Choi, I. Shin, K.-S. Jeong, *J. Am. Chem. Soc.* **2001**, *123*, 1258–1259; g) S.-S. Sun, C. L. Stern, S. T. Nguyen, J. T. Hupp, *J. Am. Chem. Soc.* **2004**, *126*, 6314–6326; h) Z. Qin, M. C. Jennings, R. J. Puddephat, *Inorg. Chem.* **2002**, *41*, 3967–3974; i) F. A. Cotton, C. Lin, C. A. Murillo, *Inorg. Chem.* **2001**, *40*, 478–484; j) E. Stulz, S. M. Scott, A. D. Bond, S. J. Teat, J. K. M. Sanders, *Chem. Eur. J.* **2003**, *9*, 6039–6048.

[4] a) P. Thanasekaran, R.-T. Liao, Y.-H. Liu, T. Rajendran, S. Rajagopal, K.-L. Lu, *Coord. Chem. Rev.* **2005**, *249*, 1085–1110; b) P. S. Mukherjee, K. S. Min, A. M. Arif, P. J. Stang, *Inorg. Chem.* **2004**, *43*, 6345–6350; c) C. J. Kuehl, S. D. Huang, P. J. Stang, *J. Am. Chem. Soc.* **2001**, *123*, 9634–9641; d) K.-S. Jeong, Y. L. Cho, S.-Y. Chang, T.-Y. Park, J. U. Song, *J. Org. Chem.* **1999**, *64*, 9459–9466; e) R. Lin, J. H. K. Yip, K. Zhang, L. L. Koh, K.-Y. Wong, K. P. Ho, *J. Am. Chem. Soc.* **2004**, *126*, 15852–15869; f) K. D. Benkstein, J. T. Hupp, C. L. Stern, *Angew. Chem.* **2000**, *112*, 3013–3015; *Angew. Chem. Int. Ed.* **2000**, *39*, 2891–2893; g) P. H. Dinolfo, M. E. Williams, C. L. Stern, J. T. Hupp, *J. Am. Chem. Soc.* **2004**, *126*, 12989–13001; h) M. Fujita, M. Aoyagi, F. Ibukuro, K. Ogura, K. Yamaguchi, *J. Am. Chem. Soc.* **1998**, *120*, 611–612; i) A. Company, L. Gómez, J. M. López Valbuena, R. Mas-Ballesté, J. Benet-Buchholz, A. Llobet, M. Costas, *Inorg. Chem.* **2006**, *45*, 2501–2508; j) C. Addicott, I. Oesterling, T. Yamamoto, K. Müllen, P. J. Stang, *J. Org. Chem.* **2005**, *70*, 797–801; k) N. Das, P. S. Mukherjee, A. M. Arif, P. J. Stang, *J. Am. Chem. Soc.* **2003**, *125*, 13950–13951.

[5] a) D. E. Janzen, K. N. Patel, D. G. VanDerveer, G. J. Grant, *Chem. Commun.* **2006**, 3540–3542; b) D. Kim, J. H. Paek, M.-J. Jun, J. Y. Lee, Sa. O. Kang, J. Ko, *Inorg. Chem.* **2005**, *44*, 7886–7894; c) C. Addicott, N. Das, P. J. Stang, *Inorg. Chem.* **2004**, *43*, 5535–5538; d) A. Hori, K. Kumazawa, T. Kusukawa, D. K. Chand, M. Fujita, S. Sakamoto, K. Yamaguchi, *Chem. Eur. J.* **2001**, *7*, 4142–4149.

[6] a) F. M. Raymo, J. F. Stoddart in *Molecular Catenanes, Rotaxanes and Knots* (Eds.: J. P. Sauvage, C. Dietrich-Buchecker), Wiley-VCH, Weinheim, **1999**, pp. 143–176; b) Y. Liu, P. A. Bonvallet, S. A. Signon, S. I. Khan, J. F. Stoddart, *Angew. Chem.* **2005**, *117*, 3110–3115; *Angew. Chem. Int. Ed.* **2005**, *44*, 3050–3055.

[7] a) M. Chas, E. Pía, R. Toba, C. Peinador, J. M. Quintela, *Inorg. Chem.* **2006**, *45*, 6117–6119; b) M. Chas, V. Blanco, C. Peinador, J. M. Quintela, *Org. Lett.* **2007**, *9*, 675–678. *N*-Monoalkyl-4,4′-bipyridinium derivatives have been used in rotaxane synthesis, see: c) S. J. Loeb, J. Tiburcio, S. J. Vella, *Chem. Commun.* **2006**, 1598–1600; d) S. J. Loeb, D. A. Tramontozzi, *Org. Biomol. Chem.* **2005**, *3*, 1393–1401.

[8] The syntheses of ligands **1** and **2** and metallocycles **7a,b** and **8a,b** was described in a previous work: M. Chas, C. Platas-Iglesias, C. Peinador, J. M. Quintela, *Tetrahedron Lett.* **2006**, *47*, 3119–3122. The syntheses of ligand **3** and metallocycles **9a,b** are described in ref. [7a].

[9] a) C. S. Johnson, Jr., *Prog. Nucl. Magn. Reson. Spectrosc.* **1999**, *34*, 203–256; b) P. Stilbs, *Anal. Chem.* **1981**, *53*, 2135–2137; c) K. F. Morris, C. S. Johnson, Jr., *J. Am. Chem. Soc.* **1992**, *114*, 3139–3141; d) For a review on the application of diffusion measurements in supramolecular chemistry, see: Y. Cohen, L. Avram, L. Frish,

Angew. Chem. **2005**, *117*, 524–560; *Angew. Chem. Int. Ed.* **2005**, *44*, 520–554.

[10] M. Fujita, S. Nagao, K. Ogura, *J. Am. Chem. Soc.* **1995**, *117*, 1649–1650.

[11] a) B. Manimaran, L.-J. Lai, P. Thanasekaran, J.-Y. Wu, R.-T. Liao, T.-W. Tseng, Y.-H. Liu, G.-H. Lee, S.-M. Peng, K.-L. Lu, *Inorg. Chem.* **2006**, *45*, 8070–8077; b) M. Yoshizawa, J. Nakagawa, K. Kumazawa, M. Nagao, M. Kawano, T. Ozeki, M. Fujita, *Angew. Chem.* **2005**, *117*, 1844–1847; *Angew. Chem. Int. Ed.* **2005**, *44*. 1810–1813; c) Y. Liu, A. H. Flood, R. M. Moskowitz, J. F. Stoddart, *Chem. Eur. J.* **2005**, *11*, 369–385.

[12] a) M. Fujita, F. Ibukuro, K. Yamaguchi, K. Ogura, *J. Am. Chem. Soc.* **1995**, *117*, 4175–4176; b) C. J. Kuehl, S. D. Huang, P. J. Stang, *J. Am. Chem. Soc.* **2001**, *123*, 9634–9641.

[13] a) A. D. Becke, *J. Chem. Phys.* **1993**, *98*, 5648–5652; b) C. Lee, W. Yang, R. G. Parr, *Phys. Rev. B* **1988**, *37*, 785–789; c) Gaussian 03, Revision C0.1, M. J. Frisch, G. W. Trucks, H. B. Schlegel, G. E. Scuseria, M. A. Robb, J. R. Cheeseman, J. A. Montgomery, Jr., T. Vreven, K. N. Kudin, J. C. Burant, J. M. Millam, S. S. Iyengar, J. Tomasi, V. Barone, B. Mennucci, M. Cossi, G. Scalmani, N. Rega, G. A. Petersson, H. Nakatsuji, M. Hada, M. Ehara, K. Toyota, R. Fukuda, J. Hasegawa, M. Ishida, T. Nakajima, Y. Honda, O. Kitao, H. Nakai, M. Klene, X. Li, J. E. Knox, H. P. Hratchian, J. B. Cross, C. Adamo, J. Jaramillo, R. Gomperts, R. E. Stratmann, O. Yazyev, A. J. Austin, R. Cammi, C. Pomelli, J. W. Ochterski, P. Y. Ayala, K. Morokuma, G. A. Voth, P. Salvador, J. J. Dannenberg, V. G. Zakrzewski, S. Dapprich, A. D. Daniels, M. C. Strain, O. Farkas, D. K. Malick, A. D. Rabuck, K. Raghavachari, J. B. Foresman, J. V. Ortiz, Q. Cui, A. G. Baboul, S. Clifford, J. Cioslowski, B. B. Stefanov, G. Liu, A. Liashenko, P. Piskorz, I. Komaromi, R. L. Martin, D. J. Fox, T. Keith, M. A. Al-Laham, C. Y. Peng, A. Nanayakkara, M. Challacombe, P. M. W. Gill, B. Johnson, W. Chen, M. W. Wong, C. Gonzalez, J. A. Pople, Gaussian, Inc., Wallingford CT, **2004**.

[14] P. J. Hay, W. R. Wadt, *J. Chem. Phys.* **1985**, *82*, 270–283.

[15] a) C. A. Hunter, J. K. M. Sanders, *J. Am. Chem. Soc.* **1990**, *112*, 5525–5534; b) J. H. Williams, *Acc. Chem. Res.* **1993**, *26*, 539–598; c) C. Bonnefous, N. Bellec, R. P. Thummel, *Chem. Commun.* **1999**, 1243–1244; d) C. G. Claessens, J. F. Stoddart, *J. Phys. Org. Chem.* **1997**, *10*, 254–272.

[16] a) C. D'Acerno, G. Doddi, G. Ercolani, P. Mencarelli, *Chem. Eur. J.* **2000**, *6*, 3540–3546; b) K. N. Houk, S. Menzer, S. P. Newton, F. M. Raymo, J. F. Stoddart, D. J. Williams, *J. Am. Chem. Soc.* **1999**, *121*, 1471–1487.

[17] The distances between H2/H6 (8.4 Å) and H3/H7 (8.4 Å) in compound **13** are longer than the cavity (7.0 Å), which precludes C−H···π interactions with these protons.

[18] The H···O and C···O distances and C−H···O angles for the four hydrogen bonds are 2.59 Å and 3.41 Å, 145°; 2.60 Å and 3.55 Å, 176°; 2.56 Å and 3.48 Å, 163°; 2.56 Å and 3.31 Å, 137°.

[19] a) K. A. Connors, *Binding Constants*, Wiley, New York, **1987**; b) H.-J. Schneider, A. K. Yatsimirsky, *Principles and Methods in Supramolecular Chemistry*, Wiley, New York, **2000**.

[20] D. B. Amabilino, P. L. Anelli, P. R. Ashton, G. R. Brown, E. Córdova, L. A. Godínez, W. Hayes, A. E. Kaifer, D. Philp, A. M. Z. Slawin, N. Spencer, J. F. Stoddart, M. S. Tolley, D. J. Williams, *J. Am. Chem. Soc.* **1995**, *117*, 11142–11170.

[21] P. L. Anelli, P. R. Ashton, R. Ballardini, V. Balzani, M. Delgado, M. T. Gandolfi, T. T. Goodnow, A. E. Kaifer, D. Philp, M. Pietraskiewicz, L. Prodi, M. V. Reddington, A. M. Z. Slawin, N. Spencer, J. F. Stoddart, C. Vicent, D. J. Williams, *J. Am. Chem. Soc.* **1992**, *114*, 193–218.

[22] L. G. Longsworth, *Phys. Chem.* **1960**, 1914–1917.

[23] R. Prins, F. J. Reinders, *Chem. Phys. Lett.* **1969**, *3*, 45–48.